# THE LOCAL ENVIRONMENTS OF LOW-REDSHIFT QUASARS AND POWERFUL RADIO GALAXIES

ERIC P. SMITH<sup>1,2</sup>

Laboratory for Astronomy and Solar Physics, Goddard Space Flight Center

AND

## T. M. HECKMAN<sup>1,3</sup>

Department of Physics and Astronomy, Johns Hopkins University, and Space Telescope Science Institute Received 1989 March 31; accepted 1989 June 27

#### **ABSTRACT**

We have studied the local environments  $(r < 100h^{-1} \text{ kpc})$  of 31 low-redshift (z < 0.3) QSOs and 35 powerful radio galaxies (PRGs—defined to have  $P_{178} > 10^{25} \text{ W Hz}^{-1}$ ) using V and R CCD frames processed through FOCAS to generate catalogs of companion galaxies. We find that the PRGs and the radio-loud QSOs typically inhabit regions with local galaxy densities similar to normal giant ellipticals and 3–4 times less dense than the regions inhabited by lower power radio-loud elliptical galaxies. The radio-loud QSOs and PRGs have about twice the average number of bright  $(L > 0.2 L_*)$ , nearby (r < 100 kpc) companion galaxies (at the 95% confidence level) compared to the radio-quiet QSOs, with the respective averages being about two companions and one companion. The luminosity function of the companions of the radio-loud objects (PRGs and QSOs) is unusually flat at the high end  $(>0.2 L_*)$  compared to a standard Schechter function (a 99% confidence level difference), while the luminosity function of the companions to the radio-quiet QSOs is consistent with a Schechter function. The brightest companion galaxy is on-average about 2 mag less bright than the QSO host galaxy or PRG (reflecting the large optical luminosities of the QSO hosts and PRGs). Finally, we find no difference between the local environments of radio-loud QSOs and PRGs in terms of galaxy density or the shape of the companion galaxy luminosity function.

These results have some interesting implications for theories of the origin of nuclear activity and the relationships between the various classes of active galaxies and QSOs. Radio-quiet and radio-loud QSOs must be intrinsically different polulations without any obvious evolutionary connection. This agrees with previously reported differences between the properties of the host galaxies. In contrast, the radio-loud QSOs and PRGs are likely to be closely related objects. They could be related in an evolutionary sense or might differ only in their geometric orientation with respect to the line of sight.

Subject headings: galaxies: clustering — quasars — radio sources: galaxies

### I. INTRODUCTION

One of the most perplexing questions regarding active galactic nuclei concerns the relationship of QSOs to powerful radio galaxies (galaxies with  $P_{178} \geq 10^{25}$  W Hz<sup>-1</sup> for  $H_0 = 100$  km s<sup>-1</sup> Mpc<sup>-1</sup>, hereafter denoted PRGs). Detailed investigations of the QSOs and PRGs have found many common features, such as radio power and radio morphology, regions of both broad-line and narrow-line optical emission, host galaxies with unusual optical morphologies and colors, and large amounts of infrared emission (Smith *et al.* 1986, SHBRB hereafter; Hutchings 1987; Soifer, Houck, and Neugebauer 1987; Golombek and Miley 1988; Smith and Heckman 1989a, b).

Many investigators of the host galaxies of QSOs (Hutchings, Crampton, and Campbell 1984, HCC hereafter; Malkan 1984; SHBRB) have suggested that radio-loud (RL) QSOs have host galaxies which exhibit surface brightness profiles best fitted by  $r^{1/4}$  law light distributions—similar to elliptical galaxies. HCC and SHBRB also report that a large fraction ( $\sim 50\%$ ) of the

" $r^{1/4}$  law" galaxies appear morphologically distorted. Until recently, it was believed that PRGs were all normal giant elliptical galaxies. However, Heckman *et al.* (1986), and Smith and Heckman (1989b) have demonstrated that a significant fraction ( $\sim 50\%$ ) of those PRGs with strong optical emission lines in their spectra are morphologically distorted galaxies.

Although the host galaxies of QSOs and PRGs (which we shall hereafter refer to as active galaxies) have been extensively studied and compared, a comparison of their local environments may prove helpful in determining the nature of their relationship (if any). For many years it has been known that the environment can profoundly affect active galaxies (for a review see Balick and Heckman 1982). Previous studies of the local environments of active galaxies have discerned one clear trend: an unusually high density of galaxies near the active galaxy (see, e.g., Stockton 1978; Longair and Seldner 1979; Gehren et al. 1984; Yee and Green 1984; Heckman, Carty, and Bothun 1985; Prestage and Peacock 1988; Hintzen, Romanishin, and Valdes 1988). In particular, Longair and Seldner (1979) found interesting correlations between the local environments of radio galaxies and radio loud (RL) QSOs.

Given their strong resemblances to each other it is tempting to either link PRGs with QSOs (and in particular RL QSOs) in an evolutionary relationship, or view them as varying degrees of the same phenomena. For example, Barthel (1989) has sug-

<sup>&</sup>lt;sup>1</sup> Visiting Astronomer at the Kitt Peak National Observatory and Cerro Tololo Inter-American Observatory of the National Optical Astronomy Observatories, which is operated by Associated Universities for Research in Astronomy, Inc., under contract to the National Science Foundation.

<sup>&</sup>lt;sup>2</sup> National Research Council/Postdoctoral Fellow

<sup>&</sup>lt;sup>3</sup> On leave of absence from the Astronomy Program, University of Maryland.

gested that RL QSOs and PRGs are drawn from the same parent population, with the observer's viewing angle being down the radio jet (QSOs) or perpendicular to the jet (PRGs). Another example of a unifying scenario is the currently popular theory that the formation of both these types of active galaxies involves the collision or merger of two galaxies, at least one of which is a spiral (e.g., HCC; Heckman et al. 1986). Complicating this relatively simple scenario, however, are the radio-quiet QSOs and those PRGs with weak or no optical emission lines in their spectra (WE PRGs). The latter differ significantly from both the PRGs with strong optical emission (SE PRGs) and RL QSOs, bearing rather a closer resemblance to brighter cluster galaxies. Indeed many low-redshift WE PRGs are brightest cluster galaxies (BCGs); e.g., 3C 264 (A1367), 3C 317 (A2052), 3C 338 (NGC 6166), and M87 (Virgo).

We have therefore undertaken an investigation of the local environments of these various classes of active galaxy (RL and RQ QSOs, SE and WE PRGs), concentrating on the properties of the associated galaxies. In this paper we consider the "local" environment of the active galaxy to be the area projected within  $100h^{-1}$  kpc of the active galaxy nucleus. This region was chosen because (a) it has been determined observationally (Stockton 1978; Heckman et al. 1984) that galaxies within this projected region are much more likely to be associated with (i.e., at the same redshift as) the active galaxy, and (b) theoretically we would expect that it is galaxies within this region that would have a significant influence on the active galaxy-given the results which suggest that galaxy-galaxy interactions produce dramatic changes in their participants when  $v_{\rm rel} \le 300-400$  km s<sup>-1</sup>, and that these changes typically remain visible for  $10^{8-9}$  yr. The samples of QSOs and PRGs are roughly matched in redshift, with all galaxies lying in the range 0.01 < z < 0.33 (Fig. 1), but the QSO sample has a higher mean redshift (0.203) than the PRG sample (0.123). Our samples are drawn from previous studies (SHBRB; Smith and Heckman 1989a) which were primarily concerned with the active galaxy itself. The absolute magnitudes of the host galaxies of the QSOs and the PRGs are similar, though this was

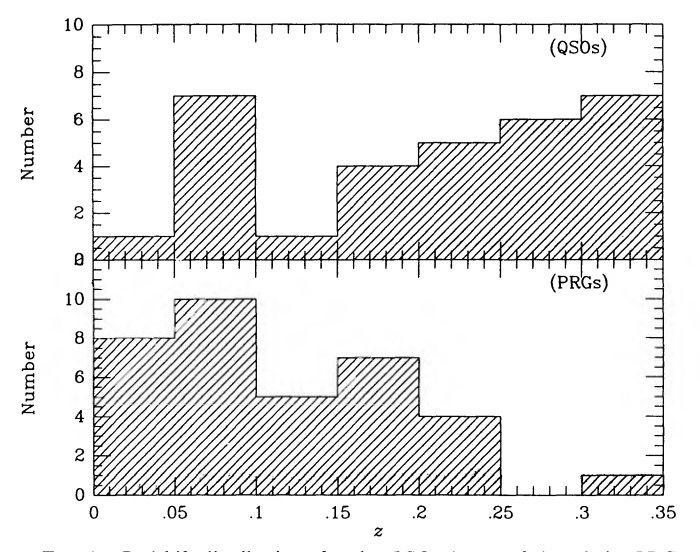


Fig. 1.—Redshift distributions for the QSOs (upper plot) and the PRGs (lower plot).

not an original selection criterion, but rather a determination from subsequent work.

In § II we discuss our observations and methods of data reduction. Our results are presented in § III. We conclude with § IV, a summary and discussion.

#### II. OBSERVATIONS AND DATA ANALYSIS

## a) Observations

The QSO data were initially acquired for a study of the nebulosity surrounding low-redshift quasars (SHBRB). These images had been obtained during four nights in 1983 June using the RCA CCD at the prime focus of the CTIO 4 m. This CCD has a 0.6 pixel<sup>-1</sup> scale and a  $3.5 \times 5.1$  total field of view. Thirty-minute exposures in the V bandpass were taken of each field. Observing conditions were photometric and the seeing was good (mean seeing 1.2 FWHM). Typical sky brightness levels ranged from 21.2 to 21.6 V mag arcsec<sup>-2</sup>, with a mean noise level of 26.8 V mag arcsec<sup>-2</sup>.

Our PRG data were originally obtained for a study of the morphological and photometric properties of these galaxies (Smith and Heckman 1989a, b). The PRG images were taken during several observing sessions: 1985 June, 1985 December, 1986 April with the CTIO (June) and KPNO 4 m (December and April) telescopes and a CCD mounted at the prime focus. We again employed the RCA CCD at CTIO, but used an  $800 \times 800$  pixel TI chip binned in a  $2 \times 2$  mode (yielding  $400 \times 400$  "big pixels" each with a size of 0.6 for the KPNO observing sessions. As with the previously obtained QSO data, images from CTIO were in V only. During the 1985 December and 1986 April sessions some images were taken in V and some in R. The R band frames were later corrected to V assuming (V-R) = 0.6 in the galaxy rest frame (Smith and Heckman 1989a). With the exception of one night of CTIO observations, conditions were photometric and seeing ranged from 1".0 < FWHM < 2".4. For our PRG images, which were exposures of typically 10 or 15 minutes, the mean sky background was 21.1 V mag arcsec<sup>-2</sup>, with a mean noise level of 25.6 V mag

Data frames were all bias-subtracted to remove the DC component of the image and flat-fielded using an image of an illuminated spot inside the domes. For the KPNO frames flatfielding was good and no fringes were visible. Fringing in several of the CTIO frames was removed from the images using the CTIO library of fringe frames. The data were calibrated using images of standard stars observed the same night. Galactic extinction corrections were made using either the H I maps of Burstein and Heiles (1982) assuming  $A_V = 3.0 \text{E}(B - V)$ or, in those cases for which we suspected that the H I map estimates of the extinction were underestimating the true extinction (3C 105 and 3C 353), the IRAS SKYFLUX plates and the results of de Vries and LePoole (1985) and Laureijs, Mattila, and Schnur (1987) assuming  $I_v(100 \mu m)/A_B = 6.3-8$ MJy sr<sup>-1</sup> mag<sup>-1</sup>. QSO host galaxy magnitudes and PRG magnitudes have been corrected for the presence of nonstellar emission in the form of point sources, nonstellar continua, or emission lines using published spectra, narrow-band images, or our own models. See Smith and Heckman (1989a) and SHBRB for details of this process.

## b) FOCAS and Data Reduction

We used the FOCAS package (Valdes 1982a) to perform our galaxy classifications, position measurements, and photo-

40

metry. The entire fields were processed, but only objects located beyond a radius equal to the 25 V mag arcsec<sup>-2</sup> isophotal radius of the active galaxy were kept for further analysis, unless inspection of the frame indicated that a galaxy was clearly discernible within that radius, e.g., 3C 75. Objects are classified according to templates constructed from the image point-spread function (PSF). The templates are fitted to each object detected, and a Bayesian classification scheme is used to determine the fit with the maximum likelihood. These templates are given by Valdes (1982b) as

$$t(r_i) = \beta s(r_i/\alpha) + (1 - \beta)s(r_i) ,$$

where  $r_i$  is the location of pixel i,  $\alpha$  is a scale factor, and  $\beta$ represents the amount of broadened intensity added to a stellar template  $s(r_i)$ . With this parameterization, resolved objects (i.e., galaxies) will have  $\alpha > 1$ . For these analyses two or more stars in each frame were chosen to construct the point-spread function for that particular frame. The default settings of the image resolution classifier were used to separate objects into the various classes recognized by FOCAS (stars, galaxies, noise, diffuse). Hence, those objects whose scales were smaller than 0.8 × PSF were classed as noise, objects with scales in the range 0.81-1.20 × PSF were considered stars, objects with scales 1.21-5.00 × PSF were classified as galaxies. Larger objects, when not merged groups of smaller objects, were classified as diffuse (these were always low-level flat-fielding problems). These scale values typically yield good separation between galaxies and stars when seeing is good (Valdes 1982b; Hintzen, Romanishin, and Valdes 1988). Objects classified as galaxies, but whose isophotal areas (the total number of pixels in the object more than  $3\sigma_{sky}$  above sky background in our case) were smaller than 25 contiguous pixels, were discarded in subsequent analyses. Individual frames were then inspected to verify the classification of faint objects.

Reported magnitudes for the FOCAS galaxies are determined from the total luminosity calculated by the program. FOCAS calculates the total area by summing pixels from the filled-in concavities in the object detection isophote and then adds successive rings—concentric with the outer isophote—until the area exceeds the detection area by a preset factor, which in our case was 2. The counts within this area are summed to give a total luminosity. This number is converted to an instrumental magnitude and later corrected to our photometric scale. Absolute magnitudes were determined, assuming  $H_0 = 100 \, \mathrm{km \, sec^{-1} \, Mpc^{-1}}, q_0 = 0$ , by

$$M_V = m_V - 42.384 - 5 \log [z(1 + z/2)] - K(z)$$
,

where K(z) is the cosmological K correction taken from Bruzual (1983) for ellipticals and Pence (1976) for spirals for the active galaxies. A mean K correction for galaxies believed to be associated with the active galaxy was determined by assuming a standard mix of spirals and ellipticals (70%–30%) and using this ratio for the galaxies in each field. We note that this ratio of spirals to ellipticals may overestimate the abundance of spirals in clusters, but will later show (§ III) that this overestimation is a small effect for the properties under consideration. The basic observational data are summarized in Table 1.

## III. RESULTS

## a) Background Determination

The accurate estimation of the number of background galaxies within the region of interest is critical to our determination of the properties of associated galaxies. Because we have redshift measurements for only the active galaxy itself, we must remove the background galaxies in a statistical manner. Previous studies using this type of correction (e.g., Yee and Green 1984) have relied on control fields observed some distance from the active galaxy. We have no control frames, and instead chose to estimate the background galaxy density in two independent ways: from the outer parts of our data frames and from published galaxy counts.

Earlier studies of the neighborhoods of QSOs (Stockton 1978; HBBS; Yee and Green 1984) determined that beyond a radius of  $\sim 100$  kpc from the active galaxy the likelihood of a galaxy being associated with the QSO drops greatly. Therefore, we measured our backgrounds from areas of the CCD which were more distant than 100 kpc (in projection) from the active galaxy using only the fields whose active galaxy had  $z \geq 0.2$ . Sampling the field in circular annuli starting at a radius of 100 kpc and reaching to 300 kpc typically allowed us to examine regions 10–12 square arcminutes in size to estimate backgrounds. Galaxies within these regions whose isophotal areas were greater than 25 contiguous pixels, and whose total magnitude was brighter than 24 V mag were binned in 1 magnitude intervals.

In Figure 2 we present our findings for the magnitude distribution of galaxies brighter than 24 V mag along with the similar determinations from Tyson and Jarvis (1979) and Sebok (1986). We have converted the Tyson and Jarvis J magnitudes to V assuming (J-V)=0.25 (Oemler 1974), and the Sebok r data to V assuming (V-r)=0.17 (Sebok 1986). From this figure it is apparent that we follow the other data reasonably well down to about 22 V mag, after which our data become incomplete. Separate tests for the QSO (PRG) data reveal them to be complete to about 22 (21.5) V mag. We therefore adopt these values when treating the samples separately and 21.5 V mag for both the QSOs and PRGs when comparing the two samples. In subsequent analyses we shall be concerned only with galaxies brighter than the completeness limits for the two data sets.

Because the Tyson and Jarvis data set was considerably larger than ours (~68,000 objects vs. ~7000 objects), and our

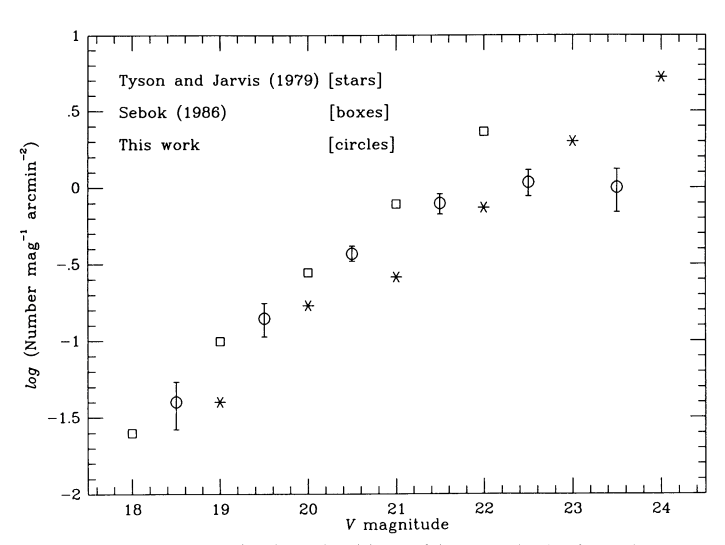


Fig. 2.—Background galaxy densities at faint magnitudes from the outer portions of CCD frames of active galaxies with z > 0.2. Similar determinations from Tyson and Jarvis (1979) and Sebok (1986) included for comparison.

TABLE 1
Basic Observational Data

Object	Emission Class <sup>a</sup>	z	$V^{b}$	Α°	K <sup>d</sup>	$K'^{d}$	Object	Radioa	z	$V^{b}$	Α°	$K^{d}$	$K'^{d}$
PRGs						QSOs							
3C 17	SE	0.220	17.69	0.03	0.22	0.34	0031-076	Q	0.291	19.69	0.00	0.59	0.53
3C 29R	WE	0.045	13.92	0.03	0.04	0.06	0037 – 061	Q	0.063	17.40	0.00	0.07	0.08
3C 33R	SE	0.060	15.39	0.00	0.06	0.08	0049 + 171	Q	0.064	18.48	0.00	0.10	0.08
3C 62	SE	0.148	16.77	0.00	0.18	0.19	0050 + 106	Q	0.061	15.55	0.00	0.07	0.08
3C 63	SE	0.175	17.95	0.00	0.14	0.24	0105 008	L	0.316	21.74	0.00	1.04	0.61
3C 75	$\mathbf{W}\mathbf{E}$	0.024	12.96	0.18	0.01	0.04	0134+033	Q	0.079	17.79	0.00	0.13	0.11
3C 78	WE	0.029	12.57	0.27	0.01	0.04	0135 - 057	L	0.308	20.51	0.00	1.02	0.58
3C 89R	WE	0.139	16.35	0.15	0.10	0.18	0137 + 012	L	0.260	18.12	0.00	0.30	0.45
3C 98R	SE	0.031	14.12	0.41	0.03	0.04	0137 – 057	L	0.330	20.02	0.00	0.90	0.65
3C 105R	SE	0.089	15.96	> 2.00	0.06	0.20	0146+089	Q	0.270	19.74	0.00	0.52	0.47
3C 109	SE	0.306	18.20	0.72	0.43	0.58	0157+001	Q	0.164	16.28	0.00	0.25	0.22
3C 171	SE	0.238	18.32	0.21	0.26	0.38	0205+024	Q	0.155	19.19	0.00	0.29	0.20
3C 192	SE	0.060	15.70	0.00	0.04	0.07	0213 – 484	Q	0.168	18.75	0.00	0.26	0.23
3C 196.1	SE	0.198	16.71	0.09	0.18	0.29	0231 + 022	L	0.322	19.89	0.00	0.69	0.63
3C 198	SE	0.082	16.88	0.03	0.05	0.11	0530 – 379	Q	0.290	19.57	0.03	0.65	0.53
3C 219	SE	0.174	16.99	0.00	0.14	0.24	0736+017	L	0.191	18.49	0.12	0.18	0.28
3C 223	SE	0.137	17.00	0.00	0.09	0.17	2130+099	Q	0.061	16.08	0.03	0.07	0.08
3C 227	SE	0.086	16.95	0.00	0.05	0.12	2135 – 147	L	0.200	17.68	0.00	0.18	0.29
3C 234	SE	0.185	17.65	0.00	0.15	0.26	2141 + 175	L	0.213	18.36	0.01	0.20	0.32
2C 236	SE	0.099	15.72	0.00	0.06	0.13	2156 – 204	Q	0.250	22.21	0.00	0.58	0.42
3C 285R	SE	0.079	15.95	0.00	0.05	0.11	2209 + 185	Q	0.070	16.25	0.03	0.04	0.09
3C 293R	WE	0.045	14.23	0.00	0.03	0.05	2214 + 139	Q	0.067	15.92	0.02	0.11	0.09
3C 300	SE	0.270	19.18	0.03	0.30	0.47	2215-037	Q	0.241	18.79	0.01	0.44	0.39
3C 305R	SE	0.042	13.75	0.00	0.03	0.05	2233 + 135	Q	0.325	21.86	0.09	0.69	0.64
3C 346	SE?	0.161	17.03	0.18	0.15	0.21	2247 + 140	Ĺ	0.237	18.91	0.02	0.84	0.38
3C 348	WE	0.154	16.26	0.18	0.10	0.20	2251 + 113	L	0.323	18.56	0.01	0.49	0.63
3C 353	WE	0.030	13.31	> 2.00	0.02	0.04	2300 – 189	L	0.129	18.39	0.17	0.10	0.16
3C 390.3	SE	0.056	15.67	0.15	0.03	0.07	2304+043	Q	0.042	15.73	0.01	0.07	0.06
3C 403	SE	0.059	14.96	0.66	0.04	0.07	2305 + 187	Ĺ	0.313	19.45	0.01	0.66	0.60
3C 424	WE	0.127	17.59	0.30	0.07	0.16	2328 + 167	L	0.284	19.70	0.09	0.97	0.51
3C 433	SE	0.102	15.98	0.33	0.06	0.13	2355 – 082	L	0.211	18.49	0.00	0.77	0.32
3C 436	SE	0.215	17.71	0.27	0.20	0.32							
3C 444	WE	0.153	15.90	0.00	0.10	0.20							
3C 445	SE	0.056	16.63	0.09	0.03	0.07							
3C 459	SE	0.220	17.71	0.09	0.22	0.34							

Notes.—Objects initially observed in R are noted with an "R" following their name.

agreement on the magnitude distribution of galaxies was good, we adopted their values when making final corrections. To estimate the expected number of background galaxies interior to the 100 kpc radius we simply multiplied the angular area of the CCD within this radius by the values from Figure 2. In cases where a "fractional galaxy" was needed we rounded up for expected values greater than n + 0.5. After binning the catalog galaxies in 1 mag intervals we randomly eliminated galaxies from each bin according to the estimated number expected for that interval. Any remaining galaxies are excess objects in the sense that their density is higher than expected for random patches of sky of the same area. It is these galaxies we deem as associated with the active galaxy. Absolute magnitudes for the associated galaxies were determined and the resulting distributions for the PRG and QSO fields are presented in Figure 3a, b. In these figures the associated galaxies are identified by hashed regions, while the dashed line represents the background + associated galaxy distribution.

# b) Clustering of Galaxies near PRGs and QSOs

## i) Previous Studies

The clustering properties of galaxies near PRGs are well documented (Longair and Seldner 1979; Stocke and Perrenod 1981; Heckman et al. 1986; Prestage and Peacock 1988). All of these studies have demonstrated that there are strong correlations between properties such as radio morphology and power, optical emission-line class, and the local galaxy density for radio galaxies. In particular, Longair and Seldner (1979) determined that powerful radio sources which also have extended radio morphologies are found in regions of space where the amplitude of the spatial cross correlation functions is 4–5 times larger than regions near randomly selected galaxies. Prestage and Peacock (1988) have carried the study further using a larger sample and more sophisticated galaxy counting techniques. For a large number of galaxies (~200 radio galaxies, though not all powerful enough to be called PRGs) in the

a Radio classification for QSOs: radio-loud (L)—radio-quiet (Q) or emission-line classification for PRGs: strong optical emission (SE)—weak/no optical emission (WE).

<sup>&</sup>lt;sup>b</sup> Apparent magnitude of the active galaxy or QSO host galaxy integrated out to the 25 V mag arcsec<sup>-2</sup> isophote. Magnitudes have been corrected for Galactic extinction, K-dimming, and nonstellar sources of emission.

<sup>°</sup> Galactic extinction values used to correct galaxy magnitudes. See § II for details.

<sup>&</sup>lt;sup>d</sup> K-correction from Bruzual 1983 or Pence 1976 for the active galaxy.

<sup>&</sup>lt;sup>e</sup> Composite K-correction for associated galaxies. See § II for details.

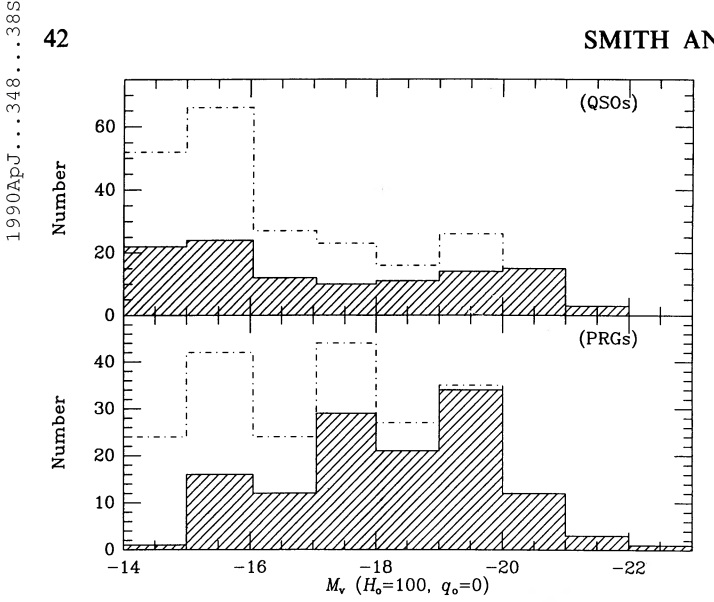


Fig. 3.—Absolute magnitude distribution of all (dot-dash line) galaxies, and galaxies remaining (hashed region) after background subtraction, in the QSO (upper plot) and the PRGs (lower plot) frames within 100 kpc of the active nucleus.

redshift range 0.015 < z < 0.25 they were able to show that radio galaxies were found in regions of space denser than field galaxies, and typical of Abell R = 0 clusters. Furthermore, they confirmed that radio galaxies with Fanaroff-Riley I radio morphologies typically inhabited regions of space about twice as dense as those with Fanaroff-Riley II (Fanaroff and Riley 1974) radio morphologies, but concluded that cluster strength alone was not responsible for the differing radio morphologies. Given the strong correlation of radio morphology with the presence of optical emission lines in radio galaxy spectra (Hine and Longair 1979) this result implies a richer environment for the WE PRGs than for the SE PRGs.

Similar clustering studies for low-redshift (z < 1) QSOs have been carried out by Yee and Green (1984, 1987) and Yee (1987). These investigations were able to show that low z QSOs are found in regions of enhanced galaxy density, but not in associations as rich as Abell R = 1 clusters. Yee and Green (1984) also found that radio-loud QSOs were found in higher density regions more frequently than radio-quiet QSOs. More specifically, the spatial covariance amplitudes for the radio-loud QSOs were nearly twice as large as those of the radio-quiet QSOs, comparable to Abell R = 0 and 4 times greater than the galaxy-galaxy covariance amplitudes (i.e., 4 times greater than for randomly selected galaxies). Yee and Green (1987) have reported, however, that there appears to be a change in the galaxy-QSO covariance function past  $z \sim 0.5$ , with the amplitude becoming larger in the past.

## ii) Our Results

As with the previous studies, we find that there are indeed more galaxies in the  $r \le 100$  kpc (projected) area than accounted for by the background galaxies. The mean total number of associated galaxies (those remaining after background subtraction, with  $m_v \le 21.5$ ) was  $3.5 \pm 0.6$  for the PRGs and  $1.6 \pm 0.3$  for the QSOs. This difference is largely due to the apparent magnitude cutoff in the sample of the associated galaxies, coupled with the larger redshift of the QSOs. The expected number of background galaxies within 100 kpc with  $m_V \le 21.5$  was 3.9 for the PRGs, and 1.9 for the QSOs. Thus for both samples we find that there are about twice as many galaxies seen in projection as would be expected.

We sought to examine whether there was any redshiftdependence in the number of associated galaxies. We restricted our search to galaxies within r = 100 kpc,  $M_V \le -18.80$ , and also compared the number and properties of galaxies associated with the QSO versus the PRGs. This limiting magnitude  $(-18.8, \sim 0.2L_{\star})$  was used because it is the faintest absolute magnitude for which our data are complete for all fields. Figure 4 shows the distribution of the number of associated galaxies with redshift. We find that there is no significant redshiftdependence in the number of (relatively bright,  $L_{\rm gal} \ge 0.2 L_{\star}$ ) galaxies associated with the PRGs (a least-squares fit to the data yields a correlation coefficient R = 0.08) over our limited redshift range (0.02  $\leq z \leq$  0.33). The QSO data show a weak correlation of number of bright associated galaxies with redshift (R = 0.35). On average the PRGs have 1.82  $\pm$  0.32 associated galaxies (with  $L_{\rm gal} \ge 0.2 L_{\star}$ ) compared with  $1.26 \pm 0.27$ for the QSOs. The weak correlation of number of bright associated galaxies with redshift with redshift will enable us to group objects, regardless their redshifts, for later comparisons. That is, we will assume that the number of bright associated galaxies remains constant over our limited redshift range.

There is however a difference in the mean number of bright galaxies associated with RL (1.81  $\pm$  0.26) objects (both QSOs and PRGs) and RQ (0.88  $\pm$  0.35) objects (significant at the 95% confidence level using a Student's t-test). On average the WE PRGs had  $2.33 \pm 0.76$  bright associated galaxies while the SE PRGs had  $1.65 \pm 0.35$  bright associated galaxies. Unfortunately, we have too few WE PRGs in the sample (nine total) to test previous results (Longair and Seldner 1979; Stocke and Perrenod 1981; Heckman et al. 1986; Prestage and Peacock 1988), suggesting that WE PRGs are preferentially found in higher density environments than SE PRGs. Properties such as the IR luminosity (measured at 60 µm), galaxy colors, and the slope of the galaxy surface brightness profile (see Smith and Heckman 1989a, b) are not correlated with the number of associated galaxies for the PRG sample.

Heckman, Carty, and Bothun (1985, HCB hereafter) analyzed a large sample (93) of low-redshift radio-loud and

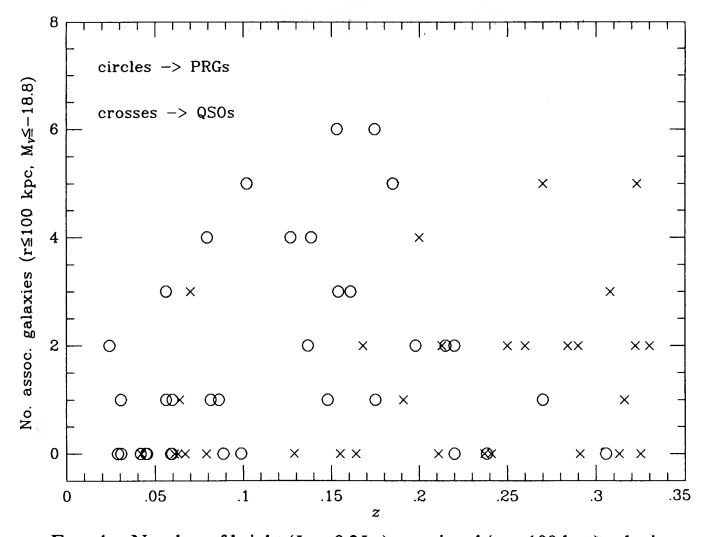


Fig. 4.—Number of bright ( $L > 0.2L_*$ ) associated (r < 100 kpc) galaxies as a function of redshift for the QSOs (x's) and the PRGs (circles).

radio-quiet ellipticals in order to study the effect of local environments on the production of radio emission. They developed a simple method for measuring the relative importance of the number, size, and proximity of neighboring galaxies. For each galaxy they constructed the following quantities:

$$\sigma_{ij} = \sum_{k} d_{k}^{-1} l_{k}^{j}, \quad i, j = 0, 1$$

where  $d_k$  is the distance of the kth galaxy from the active galaxy (in units of 100 kpc) and  $l_k$  is the luminosity of the kth galaxy relative to the active galaxy. They found that the average local density was larger by a factor of 2-3 for radio-loud ellipticals compared to radio-quiet ones. Their search area was equivalent to a circle of radius  $\sim 60h^{-1}$  kpc (in the active galaxy rest frame).

For each active galaxy in our sample we constructed  $\sigma_{ij}$ , creating measures of the total number, distance-weighted number, relative luminosity-weighted number, and both distance- and luminosity-weighted numbers for the active galaxies within a radius of 60 kpc. Note: for these measures we shall consider only those associated galaxies brighter than  $M_V = -18.8$ . (Errors introduced by the background galaxy subtraction will be smaller for the  $\sigma_{ij}$  parameters since the areas we search are smaller in angular size.) Moreover, this absolute magnitude cutoff is roughly equivalent to that used by HCB. We have also recomputed  $\sigma_{0,1}$  and  $\sigma_{1,1}$  for the PRGs and QSOs using  $L_*$  to normalize the magnitudes, removing the effects of the large intrinsic magnitudes of the active galaxies. In Table 2 we list the  $\sigma_{ij}$  for each active galaxy in our samples.

We find no significant difference between the  $\sigma_{ij}$  for the QSOs and PRGs taken as a whole. However, the mean  $\sigma_{ij}$  are smaller than the quantities derived for the low-power radio-loud ellipticals in HCB by a factor of 3–4. This is an interesting result because it implies that *powerful* radio sources are produced in galaxies which are in quite different environments from low-power radio-loud ellipticals. Indeed, the  $\sigma_{ij}$  are slightly smaller than the same quantities derived by HCB for radio-quiet ellipticals suggesting that these active galaxies are found in regions that have densities lower than that of the typical elliptical galaxy.

Tests were made to look for correlations between the  $\sigma_{ij}$  and quantities intrinsic to the active galaxy such as absolute magnitude, surface brightness profile slope, 60  $\mu$ m luminosity, and optical luminosity of the nuclear point source. No significant trends were found. In the next section we shall examine more closely the relationship of the active galaxy to its largest neighbor.

## iii) The Brightest Associated Galaxies

Theoretical investigations of galactic mergers and cannibalism (Hausman and Ostriker 1978; Villumsen 1982; Farouki, Shapiro, and Duncan 1983; Quinn 1984; Aguilar and White 1986) have demonstrated how some galaxies might grow at the expense of neighboring galaxies, stripping stars, disrupting, or even swallowing whole those galaxies that have passed too closely. The magnitude difference between the first and second brightest galaxy in a group or cluster may therefore tell us something about the evolution of the cluster or association of galaxies as well as the luminosity distribution of galaxies associated with active galaxies.

For all comparisons of galaxy magnitudes involving the active galaxy and an associated galaxy we usually used the

TABLE 2
Density Parameters

Object	$\sigma_{00}$	$\sigma_{01}$	$\sigma_{01}{}'$	$\sigma_{10}$	$\sigma_{11}$	$\sigma_{11}{}'$
3C 17	2	0.40	1.28	5.25	1.12	3.62
3C 29R	0	0.00	0.00	0.00	0.00	0.00
3C 33R	ő	0.00	0.00	0.00	0.00	0.00
3C 62	ő	0.00	0.00	0.00	0.00	0.00
3C 63	1	0.20	0.31	1.69	0.34	0.52
3C 75	2	0.62	1.56	22.01	8.88	22.31
3C 78	0	0.00	0.00	0.00	0.00	0.00
3C 89R	1	2.35	2.40	1.77	4.16	4.29
3C 98R	0	0.00	0.00	0.00	0.00	0.00
3C 105R	0	0.00	0.00	0.00	0.00	0.00
3C 109	0	0.00	0.00	0.00	0.00	0.00
3C 171	0	0.00	0.00	0.00	0.00	0.00
3C 192 3C 196.1	2 1	0.35 0.07	0.45 0.44	6.15 2.14	0.64 0.15	0.82 0.95
3C 198	0	0.07	0.00	0.00	0.13	0.93
3C 219	3	1.09	4.04	11.76	5.59	22.07
3C 223	2	0.51	1.11	6.71	1.83	4.00
3C 227	õ	0.00	0.00	0.00	0.00	0.00
3C 234	2	0.30	0.69	4.38	0.73	1.67
3C 236	0	0.00	0.00	0.00	0.00	0.00
3C 285R	1	0.52	0.95	2.47	1.30	2.38
3C 293R	1	0.06	0.17	4.51	0.27	0.76
3C 300	1	0.25	0.32	2.30	0.57	0.73
3C 305R	0	0.00	0.00	0.00	0.00	0.00
3C 346	1	0.08	0.24	5.61	0.47	1.41
3C 348 3C 353	0	0.00	0.00	0.00 3.30	0.00	0.00
3C 353 3C 390.3	1 1	0.09 0.32	0.26 0.37	2.00	0.31 0.64	0.89 0.74
3C 403	0	0.00	0.00	0.00	0.04	0.00
3C 424	2	0.66	0.71	4.23	1.43	1.55
3C 433	4	1.66	4.99	19.01	14.32	43.05
3C 436	1	0.15	0.45	2.13	0.34	1.02
3C 444	2	0.23	1.76	4.08	0.49	3.74
3C 445	1	0.40	0.19	3.61	1.45	0.70
3C 459	0	0.00	0.00	0.00	0.00	0.00
0031 – 076	0	0.00	0.00	0.00	0.00	0.00
$0037 + 061 \dots 0049 + 171 \dots$	0 1	0.00 1.23	0.00 0.14	10.00 2.11	0.00 2.59	0.00
0050+106	0	0.00	0.00	0.00	0.00	0.00
0105-008	1	0.54	0.22	3.11	1.66	0.69
0134+033	Ô	0.00	0.00	0.00	0.00	0.00
0135-057	0	0.00	0.00	0.00	0.00	0.00
$0137 + 012 \dots$	2	0.06	0.24	6.51	0.20	0.74
0137-010	0	0.00	0.00	0.00	0.00	0.00
$0146 + 089 \dots$	3	0.69	0.79	11.08	2.64	2.99
0157+001	0	0.00	0.00	0.00	0.00	0.00
0205+024	0	0.00	0.00	0.00	0.00	0.00
0213-484	2	1.20	0.94	5.37	3.22	2.53
$0231 + 022 \dots \dots 0530 - 379 \dots \dots$	1 1	0.22	0.37	2.25	0.49	0.84
0006 040	0	0.09 0.00	0.16	3.71	0.32	0.58
$0/36 + 017 \dots \dots 2130 + 099 \dots \dots$	0	0.00	0.00	0.00	0.00	0.00
2135-147	2	0.14	0.41	4.37	0.35	0.99
2141 + 175	0	0.00	0.00	0.00	0.00	0.00
2156 – 204	Ö	0.00	0.00	0.00	0.00	0.00
2209 + 185	2	0.76	0.79	7.12	2.79	2.91
2214+139	0	0.00	0.00	0.00	0.00	0.00
2215-037	0	0.00	0.00	0.00	0.00	0.00
2233+135	0	0.00	0.00	0.00	0.00	0.00
2247 + 140	0	0.00	0.00	0.00	0.00	0.00
2251+113	2	0.24	1.17	4.56	0.46	2.26
2300 – 189	0	0.00	0.00	0.00	0.00	0.00
2304+043 2305+187	0	0.00	0.00	0.00 0.00	0.00	0.00
2328+167	2	1.17	2.53	4.11	2.40	5.19
2355-082	õ	0.00	0.00	0.00	0.00	0.00

Note.—See § III for definition of  $\sigma_{ij}$ . Primed parameters have been calculated using  $M_{\star}$  to normalize associated galaxy fluxes; see § III.

1990ApJ...348...38S

TABLE 3 PROPERTIES OF ASSOCIATED GALAXIES

Object	M <sup>a</sup>	N(m) <sup>b</sup>	N(M)°	$M_{12}^{d}$	Object	M <sup>a</sup>	N(m) <sup>b</sup>	N(M)°	$M_{12}^{d}$
3C 17	-21.63	2	2	0.85	0031 – 076	-20.90	0	0	2.98
3C 29R	-21.76	0	0	6.05	0037 – 061	-19.12	1	0	2.85
3C 33R	-20.93	6	0	3.51	0049 + 171	-18.10	4	1	1.02
3C 62	-21.62	1	1	2.72	0050 + 106	-20.90	3	0	4.03
3C 63	-20.83	1	1	1.42	0105 – 008	-10.50	0	1	< 0.29
3C 75	-21.36	5	2	0.02	0134+033	-10.30	5	0	2.20
3C 78	-22.14	3	0	5.03	0135 – 057	-20.65	2	3	1.18
3C 89R	-21.89	6	4	-0.36	0137+012	-21.90	0	2	3.84
3C 98R	-20.73	1	0	3.78	0137 – 057	-21.19	2	2	< 0.75
3C 105R	-21.26	2	0	3.79	0146+089	-20.60	3	5	1.47
3C 109	-21.92	0	0	> 2.65	0157+001	-22.60	1	0	4.28
3C 171	-21.20	0	0	> 3.21	$0205 + 024 \dots$	-19.60	0	0	2.43
3C 192	-20.63	2	1	0.96	0213-484	-20.20	2	2	0.35
3C 196.1	-22.36	2	2	2.86	0231 + 022	-21.05	2	2	1.29
3C 198	-20.15	1	1	-1.30	0530 – 379	-21.10	0	2	< 2.38
3C 219	-21.78	7	6	-1.00	0736+017	-20.80	1	1	1.14
3C 223	-21.21	3	2	1.10	2130+099	-20.40	3	0	2.51
3C 227	-20.20	2	1	0.51	2135 – 147	-21.60	3	4	2.23
3C 234	-21.26	5	5	0.25	2141 + 175	-21.10	1	2	1.79
2C 236	-21.74	0	0	> 5.67	2156 – 204	-18.00	2	2	< -1.00
3C 285R	-21.02	4	4	0.65	2209 + 185	-20.50	6	3	0.62
3C 293R	-21.48	2	0	3.71	2214+139	-20.80	0	0	3.78
3C 300	-20.64	1	1	1.12	2215-037	-21.20	0	0	3.50
3C 305R	-21.77	0	0	6.06	2233 + 135	-19.19	0	0	< 2.16
3C 346	-21.56	3	3	1.39	2247 + 140	-21.45	0	0	2.45
3C 348	-22.22	7	3	3.27	2251 + 113	-22.20	4	5	1.93
3C 353	-21.51	10	1	2.49	2300 – 189	-19.95	Ó	Õ	3.05
3C 390.3	-20.52	16	3	0.76	2304+043	-19.90	4	Ō	2.93
3C 403	-21.34	2	0	0.60	2305 + 187	-21.40	0	0	2.22
3C 424	-20.45	7	4	0.16	2328 + 167	-21.30	2	2	0.32
3C 433	-21.56	8	5	0.01	2355-082	-21.50	ō	ō	5.42
3C 436	-21.56	2	2	1.72			•	•	2.12
3C 444	-22.57	8	6	1.50					
3C 445	-19.56	5	1	0.65					
3C 459	-21.61	0	Ô	3.66					
	21.01								

<sup>&</sup>lt;sup>a</sup> Absolute V magnitude of the active galaxy, corrected for Galactic extinction, K-dimming, nonstellar emission, and integrated out to the 25 V mag arcsec<sup>-2</sup> isophote.

magnitude of the active galaxy determined by FOCAS for internal consistency. Several of the active galaxies, however, are significantly influenced by the presence of nonstellar emission (chiefly in the form of stellar point sources in their nuclei). We used the corrected magnitudes for these galaxies when comparing them with those of the associated galaxies (specifically noted in Table 3—see also Smith and Heckman 1989a). For those cases where no neighboring galaxy was found (see Table 3), we used the absolute magnitude corresponding to a limiting magnitude ( $m_V = 22$ ) to assign an upper limit to  $M_{12}$ . For our sample taken as a whole we find, QSOs  $\langle M_{12} \rangle = 1.97 \pm 0.05 \text{ PRGs } \langle M_{12} \rangle = 1.98 \pm 0.06 \text{ within } 100$ kpc. Mean values have been determined using methods outlined in Feigelson and Nelson (1985) for treating censored data with the ASURV software (T. Isobe, private communication). In a study of 17 QSO host galaxies, Gehren et al. (1984) determined the magnitude difference to be  $\langle M_{12} \rangle = -1.80 \pm 0.45$ in the r band [assuming (B-r) = 0.5] for galaxies interior to  $112h^{-1}$  kpc.

There is no significant difference in the  $\langle M_{12} \rangle$  of the RQ and RL QSOs and PRGs, we find,  $\langle M_{12} \rangle_{RQ}$ : = 1.97  $\pm$  0.39 and  $\langle M_{12} \rangle_{RL} = 2.06 \pm 0.27$ . A slightly larger, though still statistically insignificant spread in  $\langle M_{12} \rangle$ , was found between the SE and WE PRGs with  $\langle M_{12} \rangle_{\rm SE} = 1.82 \pm 0.38$  and  $\langle M_{12} \rangle_{WE} = 2.43 \pm 0.76$ . For each subclass of object (RL objects, RQ objects, SE objects, etc.) we summarize the mean values for the various parameters ( $\langle M_{12} \rangle$ ,  $\sigma_{ij}$ , etc.) in Table 4.

In SHBRB we were able to determine QSO host galaxy morphologies for 16 of the QSOs. Separating the QSO sample into disk and elliptical systems we found that 11 disk-model QSO hosts have  $\langle M_{12} \rangle = 2.7 \pm 0.3$  and 5 elliptical-model QSO hosts having  $\langle M_{12} \rangle = 2.0 \pm 0.6$ . The difference, though not statistically significant, is suggestive of a Malmquist bias. Because elliptical galaxies are typically found in richer environments than spirals we might expect a smaller  $\langle M_{12} \rangle$ for those QSOs with elliptical hosts. To further examine this effect we can compare the number of bright galaxies associated with the elliptical-model galaxies and the disk-model galaxies. For the elliptical systems we find  $\langle N(M) \rangle = 3.00 \pm 0.32$  and for the disk systems  $\langle N(M) \rangle = 0.64 \pm 0.47$ . A Wilcoxon test indicates that this difference is significant at the 98.5% confidence level. Those systems found to be best modeled by an

b Number of associated galaxies within r = 100 kpc of the active galaxy nucleus and with  $m_{\rm gal} < 21.5$ .
c Number of associated galaxies within r = 100 kpc of the active galaxy nucleus and with  $M_{\rm gal} < -18.8$ .
d Magnitude difference between the active galaxy and the next brightest galaxy within 100 kpc of the active galaxy nucleus. Greaterthan limits imply no galaxy brighter than  $m_V = 22$  was found within this radius. Less-than limits indicate that only an upper limit for the magnitude of the QSO host galaxy is known.

TABLE 4
SUMMARY OF STATISTICAL PROPERTIES

Object	$\langle N(m) \rangle^{a}$	$\langle N(M) \rangle^{\rm b}$	$\langle \sigma_{00} \rangle^{c}$	$\langle \sigma_{01} \rangle$	$\langle \sigma_{10} \rangle$	$\langle \sigma_{11} \rangle$	$\langle M_{12} \rangle^{\rm d}$
PRGS QSOs RL objects RQ objects SE PRGs WE PRGs	$\begin{array}{c} 3.54 \pm 0.59 \\ 1.65 \pm 0.31 \\ 2.88 \pm 0.46 \\ 2.00 \pm 0.48 \\ 2.92 \pm 0.68 \\ 5.33 \pm 1.05 \end{array}$	$\begin{array}{c} 1.82 \pm 0.32 \\ 1.26 \pm 0.27 \\ 1.81 \pm 0.26 \\ 0.88 \pm 0.35 \\ 1.65 \pm 0.35 \\ 2.33 \pm 0.76 \end{array}$	$\begin{array}{c} 0.91 \pm 0.17 \\ 0.61 \pm 0.17 \\ 0.86 \pm 0.14 \\ 0.53 \pm 0.23 \\ 0.88 \pm 0.21 \\ 1.00 \pm 0.29 \end{array}$	$\begin{array}{c} 0.29 \pm 0.09 \\ 0.20 \pm 0.07 \\ 0.26 \pm 0.07 \\ 0.23 \pm 0.11 \\ 0.24 \pm 0.08 \\ 0.45 \pm 0.25 \end{array}$	$\begin{array}{c} 3.29 \pm 0.86 \\ 1.75 \pm 0.51 \\ 2.86 \pm 0.64 \\ 1.73 \pm 0.79 \\ 2.89 \pm 0.86 \\ 4.43 \pm 2.29 \end{array}$	$\begin{array}{c} 1.30 \pm 0.49 \\ 0.55 \pm 0.18 \\ 1.04 \pm 0.36 \\ 0.68 \pm 0.30 \\ 1.15 \pm 0.58 \\ 1.73 \pm 1.00 \end{array}$	$\begin{array}{c} 1.97 \pm 0.05 \\ 1.98 \pm 0.06 \\ 2.06 \pm 0.27 \\ 1.97 \pm 0.39 \\ 1.82 \pm 0.38 \\ 2.06 \pm 0.27 \end{array}$

Notes.—Summary of statistical properties of the sample.

- <sup>a</sup>  $\langle N(m) \rangle$  is the mean number of galaxies within r = 100 kpc with  $m_V \le 21.5$ .
- b  $\langle N(M) \rangle$  is the mean number of galaxies within r = 100 kpc with  $\dot{M}_{V} \leq -18.8$ .
- ° The  $\sigma_{ii}$  have been computed using galaxies with r < 60 kpc and with absolute magnitudes  $M_V \le -18.8$ .

<sup>d</sup> Magnitude differences,  $\langle M_{12} \rangle$ , between the active galaxy and the next brightest galaxy within r = 100 kpc with  $m_V \le 22$ .

elliptical galaxy (in SHBRB) appear to be located in richer environments compared with those objects modeled by disk galaxies.

#### iv) Luminosity Function of the Associated Galaxies

The luminosity function of the associated galaxies is of considerable interest. The presence of an active galaxy already indicates that something is very different about the system of galaxies compared with a typical cluster or group of galaxies. Is there anything else unusual about the other galaxies that might provide clues as to why this particular system of galaxies harbors an active member? To address this question in detail we constructed an average luminosity function for the QSO and PRG associated galaxies following the guidelines in Schechter (1976). In Figures 5 and 6 we reproduce these luminosity functions as well as the luminosity function for galaxies as a whole from Felten (1977) where we have used  $M_{+}(V) =$ -20.4 and  $\alpha = -5/4$ . The luminosity functions have been normalized so that the total area under each curve is identical. These two figures show that the luminosity function of the galaxies associated with the radio-loud QSOs and PRGs is unusually flat at the bright end  $(L > 0.2L_{\star})$  relative to a

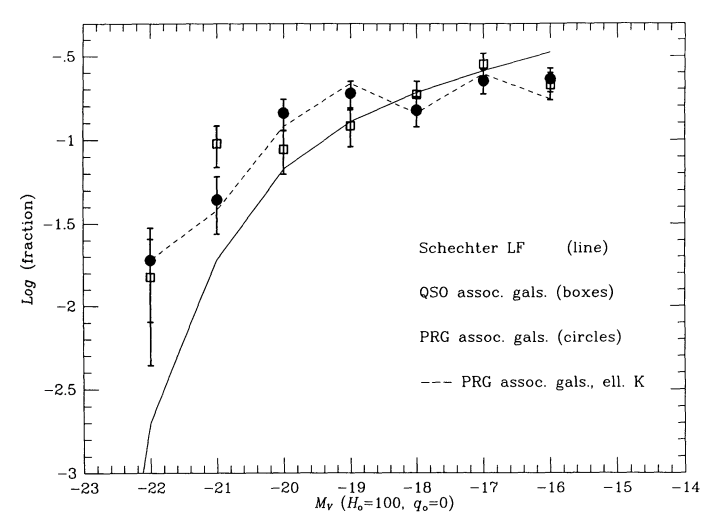


Fig. 5.—Relative luminosity functions for the QSO (squares) and PRG (filled circles) associated galaxies. A normal Schechter luminosity function  $(M_* = -20.4, \alpha = -5/4)$  has been added for comparison purposes (solid line). The dashed line represents the effect of using a purely elliptical galaxy K-correction for the PRG associated galaxies rather than the composite K-correction (see § II). All luminosity functions have been normalized to have the same integral area.

Schechter function (the difference evident in Fig 6 is found to be significant at the  $\sim 99\%$  level using a Kolmogorov-Smirnov test). A least-squares fit of a Schechter function to the radio-loud galaxy curve yields  $\alpha = -1.10$ ,  $M_*(V) = -21.9$ . On the other hand, the luminosity function of the radio-quiet QSO companions is consistent with a normal Schechter function (and also different at the  $\sim 99\%$  confidence level from the luminosity function of the galaxies associated with the radio-loud active galaxies). We also find that the luminosity functions of the companions to the radio-loud QSOs and the PRGs are statistically indistinguishable.

We have included a dashed line showing the effect of choosing a smaller K-correction for the associated galaxies in Figure 5. Having used a 70%-30% ratio of spiral to ellipticals, the adopted K-corrections were quite close to those of a spiral galaxy. To assure that this choice of K-correction was not significantly biasing our luminosity function we replotted the curve using only an elliptical galaxy K-correction (Bruzual 1983;  $\mu=0.7$  model). There is a slight shift toward fainter magnitudes, but not nearly enough to dilute the excess bright galaxies. In all cases the changes arising from choice of K-correction lie within the error bars of the associated galaxies luminosity function calculated with the composite K-correction. We therefore adopt the composite K-correction in our final estimates.

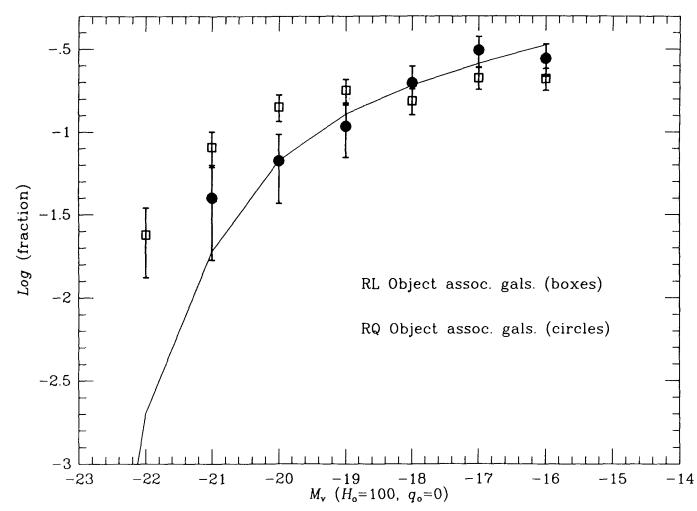


Fig. 6.—Relative luminosity functions for the RL associated objects (both QSO and PRG) plotted as squares, and the RQ, QSOs plotted as filled circles. Solid line is the normal Schechter luminosity function.

An excess of bright companion galaxies relative to a z=0Schechter function has been noted previously by Yee and Green (1987) and Hintzen, Romanishin, and Valdes (1988) for higher redshift QSOs. Both Yee and Green and Hintzen et al. found that the luminosity function undergoes a brightening by about 1 mag at redshifts  $\sim 0.6$ . In principle, the effect they found could reflect either a different shape for the luminosity function in the vicinity of QSOs or an increase in the average galaxy luminosity throughout the universe with look-back time (i.e., a shifting of  $L_*$  to larger values). In our case, the former interpretation is much more plausible. First, we see no evidence for a strong change in the luminosity function with redshift (specifically, if we divide our sample of radio-loud objects into high- and low-redshift subsets we find no significant differences. Second, the typical redshifts of our sample are so small (0.1–0.2) that a universal brightening of  $L_{\star}$  by about one magnitude due to galaxy evolution is astrophysically implausible.

#### IV. SUMMARY AND DISCUSSION

We have set out to investigate the local environments of QSOs and PRGs to search for possible similarities and differences. In the process of this examination we found that

- 1. The number of bright galaxies associated with the QSOs and PRGs implies that they are found on-average in regions only 50%-30% as dense as low-power radio galaxies. Their environments are in fact similar to (though not quite as dense as) those of average radio-quiet ellipticals.
- 2. The PRGs and RL QSOs have about twice as many bright  $(L>0.2L_*)$  companion galaxies on-average as the RQ QSOs (at the 95% confidence level). However, the number, proximity, and relative size of the bright associated galaxies do not appear to bear any important relationship to other properties (color, IR luminosity, photometric structure) of the active galaxy.
- 3.  $\langle M_{12} \rangle$ , the average magnitude difference between the active galaxy (after the luminosity associated with the activity has been removed) and the next brightest galaxy is typically 2 mag (in V).
- 4. The luminosity function of the galaxies associated with the RL objects (PRGs plus QSOs) is flatter at high luminosities ( $>0.2L_*$ ) than a standard Schechter function. This difference at the 99% confidence level is highly significant. In contrast, the luminosity function of the RQ QSOs is consistent with a Schechter function.
- 5. The environments of the RL QSOs and PRGs are statistically indistinguishable in terms of both galaxy density and shape of the luminosity functions.

These results have some interesting implications for theories of the triggering of activity in galactic nuclei and for our understanding of the relationships between the various classes of active galaxies.

The fact that about half of all the PRGs and QSOs in our sample have at least one bright  $(L > 0.2L_*)$  galaxy within a projected separation of only 60 kpc-i.e., within a few galaxy radii—is consistent with the growing body of evidence linking nuclear activity to galaxy interactions. It is also interesting in this regard that the luminosity function of the companions to the radio-loud QSOs and PRGs is enriched in bright galaxies relative to a standard Schechter function. This could result from a selection effect if the production of a powerful radio source is intially triggered by the interaction between two (or more) bright, massive galaxies. A similar effect is noted by Lauer (1989), who found that the luminosity function for second brightest galaxies in clusters has roughly the same shape as our radio-loud associated galaxies, though the apparent shift in  $L_*$  he found is less than half of that found here. Lauer (1989) attributes this brightening of the luminosity function to mild galaxy cannibalism induced via dynamical friction between the central galaxy in the cluster and nearby galaxies.

The likely differences between the environments of the radio-loud and radio-quiet QSOs implies that these two classes may not be simply related in any evolutionary sense. This is consistent with earlier work on their environments (e.g., Yee and Green 1984) and host galaxies (e.g., HCC; SHBRB). Similarly, active galaxies with very powerful radio emission (be they QSOs or radio galaxies) are evidently a distinct population from lower power ( $P_{178} \le 10^{25} \text{ W Hz}^{-1}$ ) radio galaxies. This result is also consistent with other studies of their environments (e.g., Prestage and Peacock 1988), host galaxies (e.g., Heckman et al. 1986; Smith and Heckman 1989b; Lilly and Prestage 1987), and cosmic evolution (e.g., Peacock 1985).

In contrast, the similarities between the environments and host galaxy morphologies of the radio-loud QSOs and PRGs suggest that these two classes may be closely related to one another (for a slightly different viewpoint however see Hutchings 1987). While the host galaxies of the radio-loud QSOs appear to be on-average about 0.5–1.0 magnitudes brighter than the PRGs, this result is critically dependent on an accurate decomposition of the QSOs into a point source-plusgalaxy. Hubble Space Telescope observations of radio-loud QSOs are very important to confirm this apparent difference. The present data are consistent with either an evolutionary relationship between radio-loud QSOs and PRGs, or with suggestion of Barthel (1989) that the two classes are the same population of objects viewed along (QSO) or perpendicular to (PRG) the radio jets.

E. S. wishes to thank Paul Hintzen and Frank Valdes for helpful discussions and comments, and the National Research Council for a Postdoctoral Fellowship grant. T. H. acknowledges the support of National Science Foundation grant AST 85-15896.

### **REFERENCES**

Aguilar, L. A., and White, S. D. M. 1986, Ap. J., 307, 97.
Balick, B., and Heckman, T. M. 1982, Ann. Rev. Astr. Ap., 20, 431.
Barthel, P. D. 1989, Ap. J., 336, 606.
Bruzual, G. A. 1983, Rev. Mexicana Astr. Af., 8, 63.
Burstein, D. A., and Heiles, C. 1982, A.J., 87, 1165.
de Vries, C. P., and LePoole, R. S. 1985, Astr. Ap., 145, L7.
Fanaroff, B. L., and Riley, J. M. 1974, M.N.R.A.S., 167, 31P.
Farouki, R. T., Shapiro, S. L., and Duncan, M. J. 1983, Ap. J., 265, 597.
Feigelson, E. D., and Nelson, P. I. 1985, Ap. J., 293, 192.
Felten, J. 1977, A.J., 82, 861.
Gehren, T., Fried, J., Wehinger, P. A., and Wyckoff, S. 1984, Ap. J., 278, 11.
Golombek, D., Miley, G. K., and Neugebauer, G. 1988, A.J., 95, 26.

Hausman, M. A., and Ostriker, J. P. 1978, Ap. J., 224, 320. Heckman, T. M., Bothun, G. D., Balick, B., and Smith, E. P. 1984, A.J., 89, 958. Heckman, T. M., Carty, T. J., and Bothun, G. D. 1985, Ap. J., 288, 122 (HCB). Heckman, T. M., Smith, E. P., Baum, S. A., van Breugel, W. J. M., Miley, G. K., Illingworth, G. D., Bothun, G. D., and Balick, B. 1986, Ap. J., 311, 526. Hine, R. G., and Longair, M. S. 1979, M.N.R.A.S., 188, 111. Hintzen, P., Romanishin, W., and Valdes, F. 1988, preprint. Hutchings, J. B. 1987, Ap. J., 320, 122. Hutchings, J. B., Crampton, D., and Campbell, B. 1984, Ap. J., 280, 41 (HCC). Lauer, T. R. 1989, Ap. J., submitted. Laureijs, R. J., Mattila, K., and Schnur, G. 1987, Astr. Ap., 184, 269. Lilly, S. J., and Prestage, R. M. 1987, M.N.R.A.S., 225, 531.

TIMOTHY M. HECKMAN: Physics and Astronomy Department, Johns Hopkins University, and Space Telescope Science Institute, Baltimore, MD 21218

ERIC P. SMITH: Laboratory for Astronomy and Solar Physics, Code 681, NASA/Goddard Space Flight Center, Greenbelt, MD 20771